New tools for discovering the role sRNA plays in cellular regulation

Douglas P. Shepherd[a,b]*, Nan Li[c], Elizabeth Hong-Geller[c], Brian Munsky[b,c,d]*, James H. Werner[a]*
[a]Center for Integrated Nanotechnologies, [b]Center for Nonlinear Studies, [c]Bioscience Division, [d]Computer, Computational & Statistical Sciences,
Los Alamos National Laboratory, Los Alamos, NM, USA 87545

*dpshepherd@lanl.gov; phone 1 505 606-0983
*munsky@lanl.gov; phone 1 505 665-6691
*jwerner@lanl.gov; phone 1 505 667-8842

ABSTRACT

We have used single molecule fluorescence in situ hybridization (smFISH) to study cell-to-cell heterogeneity of messenger RNA (mRNA) copy numbers for human host cells subject to a variety of external stimuli. In order to study the effect of various stimuli and genetic modifications on mRNA copy number, we have constructed an automated high-throughput multiplexed imaging system and data analysis package capable of localizing large numbers of individual mRNA transcripts in three dimensions. These experimental distributions of mRNA are used to refine and down-select regulatory models. Here we present a case example of Interleukin 1 alpha mRNA production in response to immune system stimulation. We propose a methodology for extending these methods to study the effect of small RNA on genetic expression by combining multiplexed imaging and numerical modeling at the system-level.

Keywords: smFISH, small interfering RNA, multiplex imaging, genetic expression, single molecule imaging

1. INTRODUCTION

Single molecule, single cell studies of genetic expression have provided key insights into how populations of cells respond to external stimuli. By directly measuring copy numbers of individual biomolecules in cells, such as the number of individual GFP-protein fusions, it is now possible to obtain statistical measures of the spatio-temporal distributions of key important signaling and regulatory molecules. Such comprehensive datasets can be used to create system level models that provide insight into cellular regulation, predict new behavior, and suggest new experiments that may help unravel the intricacies of a particular regulatory pathway. The combination of single-molecule spectroscopy, biochemistry, and numerical modeling is a powerful multi-disciplinary approach to investigating cellular response at the genetic level.

Multiple methods exist to fluorescently label individual messenger RNA (mRNA) transcripts[1-4]. A recent advancement by Raj, *et.al.[4]*, termed single molecule fluorescence in-situ hybridization (smFISH), enables direct detection and counting of individual endogenous mRNA transcripts, which has extended our ability to investigate the system dynamics of genetic expression. This technique has two key advantages over fluorescent protein based labeling: 1. There is no "turn-on" time for maturation as there is with GFP-based labeling[5]. 2. Directly measuring mRNA transcripts (as opposed to proteins) is one step closer to the genetic code. For many cases, the advantages of smFISH greatly outweigh the disadvantages, which are the requirement that cells are fixed and permeabilized, as well as the need for 30-50 singly labeled DNA probes, each approximately 22 nucleotides long. smFISH has emerged as a powerful research tool, being applied by multiple groups to help shed new light on genetic expression at the single transcript, single cell level [6-10].

While smFISH has been a powerful method to explore genetic expression pathways of messenger RNA that codes for proteins, we see a substantial opportunity to extend this method to explore the spatio-temporal dynamics of non-coding RNA such as small RNAs. Small RNAs (sRNA) are a recently discovered component of the genetic code, transcribed from the intergenic regions of an organism's genome[11-17]. sRNAs vary in length from a few hundred nucleotides in prokaryotes and are typically 22 nucleotides in eukaryotes. Here, we use the term sRNA to refer to small RNA expressed by prokaryotes and the term miRNA to refer to small RNA expressed by eukaryotes.

Single Molecule Spectroscopy and Superresolution Imaging V, edited by Jörg Enderlein, Zygmunt Karol Gryczynski, Rainer Erdmann, Felix Koberling, Ingo Gregor, Proc. of SPIE Vol. 8228, 822808 · © 2012 SPIE · CCC code: 1605-7422/12/$18 · doi: 10.1117/12.910540

Because of the small size (22 nucleotides) of miRNA, direct labeling and detection by the smFISH method (which typically uses 30-50 fluorescent probes per mRNA) is a substantial challenge. As such, one of our primary approaches is to use smFISH to measure mRNA that is directly affected by miRNA. To this end, we have developed a high-throughput multiplexed microscope and analysis tools capable of localizing fluorescently labeled mRNA in three dimensions within fixed, permeabilized cells.

Here, we focus on measuring and modeling the production of Interleukin 1 alpha (IL1α) mRNA in response to immune system stimulation by lipopolysaccharide (LPS). IL1α is an mRNA that is a potential target for sRNA regulation. We have also begun to extend smFISH techniques to smaller probe sets (towards the aim of direct detection of sRNA in cells) and here present results on co-localizing two spectrally distinct probe sets hybridized to individual Glyceraldehyde 3-phosphate dehydrogenase (GAPDH) mRNA transcripts.

2. EXPERIMENTS

2.1 smFISH probe sets

Probe sets were purchased from Biosearch Techonologies, utilizing a probe designer (currently in the beta-testing phase) that attempts to maximize G-C content of individual probes while ensuring minimal non-specific binding. For IL1α, Quasar 560 dye was used as the fluorescent reporter. For the split GAPDH experiments, Quasar 560 and Quasar 670 dyes were used as fluorescent reporters. Probes obtained from Biosearch Technologies were diluted in 50 mL of nuclease-free water and aliquoted into 5 mL batches for subsequent experiments.

Hybridization of the probes to target mRNA were performed in a hybridization buffer that consisted of 1 g dextran sulfate, 10 mg *Escherichia coli* tRNA, 100 mL of 200 mM Vandayl ribonucleoside complex (NEB), 40 mL of 5 mg/mL BSA (RNase free) (Ambion), 1 mL 20x saline-sodium citrate (SSC) (nuclease free, Ambion), 3 mL formamide (deionized, Ambion), with a final solution volume of 10 mL.

Washing the samples was performed in a buffer consisting of 5mL 20x SSC (RNase free, Ambion), 15 mL formamide (deionized, Ambion), and 25 mL nuclease-free water.

2.2 THP1 cell culture and fixation

Human monocytic cell line THP-1 (ATCC TIB-202) was maintained in Roswell Park Memorial Institute-1640 medium supplemented with 10% fetal bovine serum (Thermo Scientific) in a humidified 5% CO_2 atmosphere at 37°C. To induce cell differentiation and adhesion, cells ($5x10^5$ per mL) were treated with serum-free medium with 100nM phorbol 12-myristate 13-acetate (PMA) for 48 hrs on chambered #1 coverglasses (Lab-Tek, 155411). When indicated, cells were stimulated with 0.5 mg/mL lipopolysaccharide (LPS) from *Escherichia coli* 055:B5 (Sigma-Aldrich) before 3.7% formaldehyde fixation for 10 min. Cells were permeabilized in 70% ethanol overnight at 4°C before hybridization.

2.3 smFISH hybridization

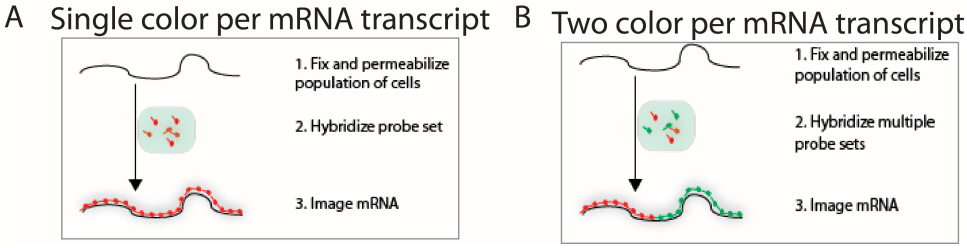

Figure 1 – Schematic of the smFISH hybridization scheme. For single color labeling (A), probes are added to fixed, permeabilized cells and then washed away. The procedure for two color labeling (B) is the same. For two color labeling, the probe concentration of the two different sets is adjusted such that the total concentration of probes (i.e. red+green) is the same as the one-color probe set.

One color IL1α mRNA: The ethanol was aspirated off and 400 mL of the wash buffer was added to each chamber. After 5 minutes, the wash buffer was aspirated and 400 mL of new wash buffer added. The probe set was then diluted in hybridization buffer to a dilution of 1:1000 (Figure 1b). 300-400 mL of probe solution was added to each chamber and incubated overnight at 30°C. In the morning, the hybridization buffer was aspirated, 400 mL of the wash buffer added to each chamber, and incubated for 30 minutes at 30°C. The wash buffer was aspirated, 400 mL of wash buffer containing 5 ng/mL of DAPI was added to each chamber, and incubated for 30 minutes at 30°C. The final wash buffer was aspirated and 400 mL of 2x SSC was added to each chamber.

Two color GAPDH mRNA: The procedure for two color labeling is identical to that of the one color labeling, with the exception that the final probe dilution (red+green probes combined) was at a final dilution of 1:1000 (Figure 1b).

2.4 Multiplexed three dimensional imaging

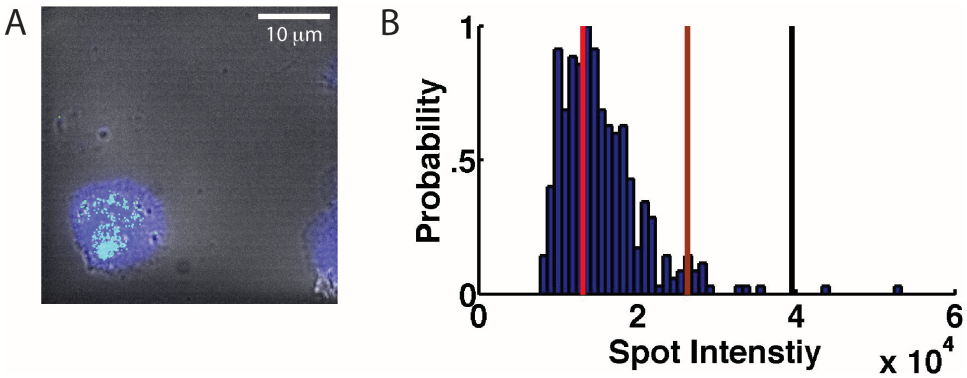

Figure 2 – A) Merged maximum Z-projection image of white light channel, DAPI channel, and IL1α smFISH channel. This cell is from of a population of cells that was fixed and permeabilized at 300 minutes post-exposure to LPS. B) Histogram of fluorescent spot intensities from the population of cells fixed and permeabilized at 300 minutes. The red line is the central value of a Gaussian fit to the first peak, the brown line is two times that central value, and the black line is three times that central value.

The imaging system is constructed on an Olympus IX71 inverted microscope. Excitation is provided by a filtered mercury arclamp (Olympus U-LH100HGAPO) and spectrally filtered by one of five Semrock filter cube sets. The filter cubes correspond to five commonly used dyes: DAPI (DAPI-1160B-000), FITC (FITC-2024B-000), Cy3 (CY3-4040C-000), Cy5 (CY5-4040C-000), and Cy7 (CY7-B-000). One of the six filter cube positions is left blank for white light imaging. The objective is an Olympus APO N 60x/1.49 TIRF oil objective and is mounted onto a Physik Instrumente Z-piezo (PI 721.20) to allow for Z sectioning through the sample. A Thor Labs MAX200 positioning stage is mounted to the microscope and a custom sample stage allows for secure mounting of eight-chamber Labtek slides. A Princeton Instruments ProEM electron-multiplying CCD (EMCCD) camera is used for image acquisition.

The positioning stage, EMCCD, and Z-piezo are all interfaced to LabVIEW through USB, GIG-E, and a digital to analog converter board, respectively. Custom LabVIEW software allows for automated collection of variable size Z-stacks at multiple areas per sample chamber. The software collects one excitation/emission channel Z-stack at a time, incrementing through the selected channels by rotating the filter turret to the appropriate cube and stepping through the Z-plane by moving the piezo. We typically take 40 steps of 250 nm in a single Z-stack for a single excitation/emission pair and collect subsequent Z stacks for other needed colors. Depending on the concentration of cells, we image between 25-100 image areas per chamber, with a step size in X and Y of 100 μm. The number of cells analyzed varies from hundreds to thousands depending on the number of image areas acquired. A typical imaging run takes 6-8 hours, followed by 2-3 days of data processing.

The data processing is completed using custom Matlab code that follows a general outline of image filtering, spot counting, image thresholding, spatial assignment for individual cells and nuclei, and finally spatial assignment of fluorescent spots to cells. Each of these tasks is completed by a sub-routine, which we describe briefly here.

Each smFISH Z-stack is first normalized, flat-field corrected, and then convolved with a three-dimensional Laplacian of a Gaussian (LOG) filter to enhance diffraction limited fluorescence spots within the Z-stack. An NVIDIA GTX 560 graphics-processing unit (GPU) is utilized to speed this step as well as other image processing steps. After the LOG filter is applied, a three-dimensional 27-member matrix (3x3x3) of zeros and ones is used in conjunction with a flood fill algorithm applied to the Z-stack to determine objects that are connected in three-dimensions [18]. Every object that meets the connected criteria is given a unique identifier and the total (normalized) intensity recorded. A threshold is then applied to all objects and the user is prompted to select a threshold where the number of spots found in the image does not significantly vary over neighboring thresholds (adapted from Raj *et.al.* [4]). A list of XYZ pixel values is generated for each fluorescence spot at or above the user-selected threshold.

After spot counting and thresholding, a maximum Z-projection image of the corresponding white light Z-stack is displayed to the user. The user then outlines every cell in the image to create the white light mask. This mask is used to automatically detect DAPI stained nuclei by automatically thresholding the corresponding DAPI Z-stack and uniquely assigning nuclei to cells. A list of XYZ pixel values is generated for each cell and nucleus defined by their respective masks. Figure 2a is a merged image showing the white light, DAPI, and filtered spots for an individual cell.

Spatial assignment of fluorescence spots is accomplished by comparing the XYZ pixel values of each fluorescence spot to the available XYZ pixel values of all cells/nuclei. If more than 80 percent of the XYZ pixels from a fluorescence spot are contained within a cell, that fluorescence spot is assigned to that cell. The XYZ pixel values for the fluorescence spot are then compared to the XYZ pixel values of the nucleus contained within that cell. If more than 80 percent of the XYZ pixels are contained within the nucleus, the spot is assigned to the nucleus. Spots that are in cells but not in the nucleus are assigned to the cytoplasm. This process is repeated until all fluorescence spots generated by the spot counting/thresholding algorithm have been assigned to cells or determined to be extra-cellular.

Finally, the total intensity of all fluorescence spots is histogrammed and the first peak is fit to a Gaussian (Figure 2b). Any fluorescence spot with a total intensity less than two times the intensity of the peak of the Gaussian (red line in Fig. 2b) is assigned as a single spot. Any spot between two to three times the intensity of the peak of the Gaussian (brown and black lines in Fig. 2b) is counted as two mRNA copies, and so on. Spots consisting of two or more mRNA transcripts inside of the nucleus are counted as transcription sites. mRNA inside of the nucleus (but not part of a transcription site) are counted separately.

For co-localization of fluorescent spots, the XYZ pixel list of every fluorescence spot in two (or more) spectrally distinct Z-stacks is compared. If more than 75 percent of the pixels are shared between two fluorescence spots, then the spot is considered co-localized. We calculate the number of spots co-localized with respect to the number of spots in each image. We report the average of these two numbers as the percentage of co-localization.

3. RESULTS

3.1 IL1α mRNA expression in response to LPS stimulation

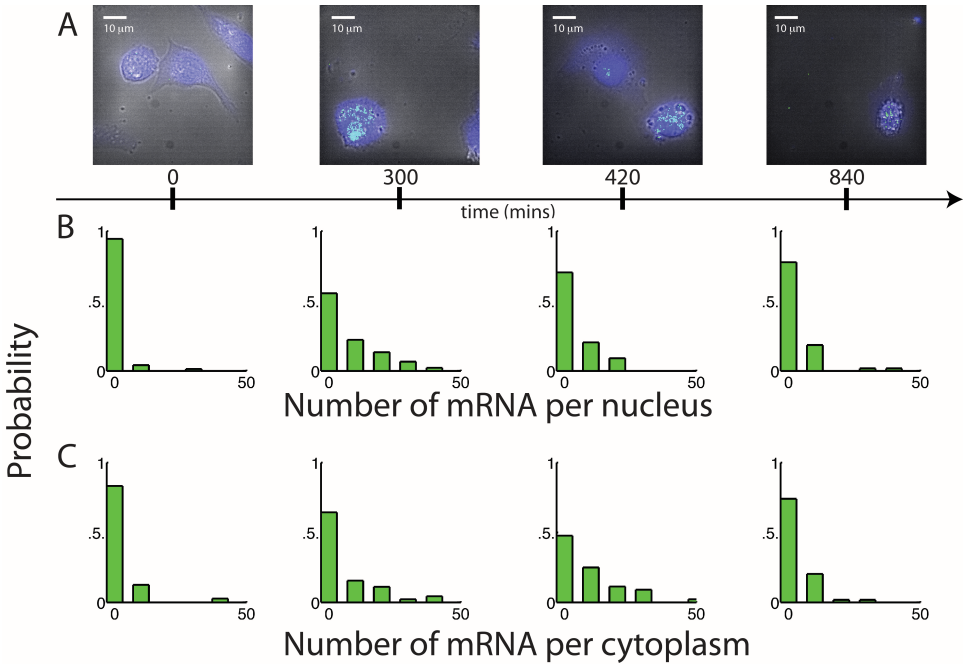

Figure 3 – A) Representative merged maximum Z-projection images from 4 of the 12 time points acquired for IL1α mRNA response. These images have been processed by our three dimensional spot finding software. The identified IL1α mRNAs are green, the nucleus is blue, and the white light image is grey. B) Normalized probability distributions of free nuclear mRNA corresponding to the same 4 time points. C) Normalized probability distributions of free cytoplasmic mRNA corresponding to the same 4 time points.

Multiple Z-stacks at twelve times points, corresponding to 0, 60, 120, 240, 360, 420, 480, 600, 720, or 840 minutes after LPS stimulation, were taken in three color channels. The white light channel is used to locate individual cells in each Z-stack, the DAPI channel is used to localize the nucleus of each cell in 3D, and a Cy3 emission channel is used to localize individual IL1α mRNA in 3D. Figure 3a shows representative merged maximum Z-projection images from four time points (0, 300, 420, and 840 minutes). A key component of the information we collect in each Z-stack is the size and intensity of every mRNA fluorescence spot. Because of this, we can assign spots brighter than the average fluorescence spot to multiple mRNAs. By localizing these spots to the nucleus, we are able to identify transcription sites. In Figure 3b and 3c, we show normalized probability distribution of mRNA localized to the nucleus and cytoplasm, respectively. Combining the information in Figure 3b and 3c, we clearly can spatially resolve the beginning of mRNA production, the migration of mRNA from nucleus to cytoplasm, and mRNA degradation. The average number of mRNA per population is shown in Figure 4. We confirmed the 3-4x increase in expression with real time PCR (RT-PCR) performed with cells from same population as those with used for the smFISH experiments.

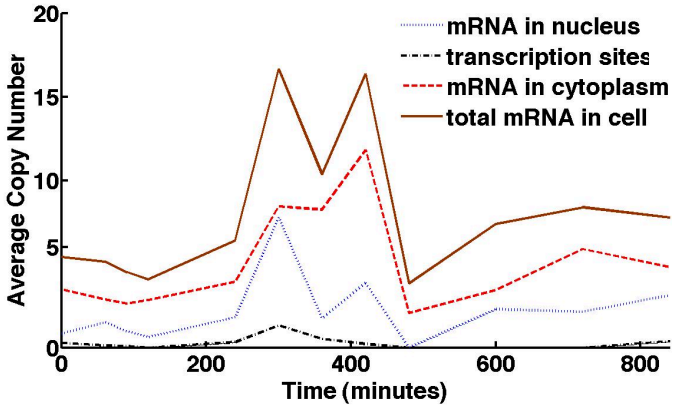

Figure 4 – Average number of IL1α mRNA and transcription sites identified over the time-course of THP1 cellular response to LPS stimulation. Production of IL1α mRNA spikes first in the nucleus, followed by diffusion to the cytoplasm.

3.2 Modeling IL1α mRNA expression in response to LPS stimulation

To quantitatively model the effects of LPS stimulation on IL1α mRNA expression, we have proposed a simple discrete stochastic model, which includes formation of transcription sites, the production of mRNA, transport of mRNA to the cytoplasm, and degradation. This stochastic model consists of four biochemical species: (i) inactive transcription sites, g_{off}; (ii) active transcription sites, g_{on}; (iii) mRNA in the nucleus $mRNA_{Nuc}$; and (iv) mRNA in the cytoplasm, $mRNA_{Cyt}$. Populations in these species change according to the reactions:

Reaction	Reaction Type	Rate Parameter (fitted)	Best Fit Values
$g_{off} \rightarrow g_{on}$	Gene activation	$k_{12} = \begin{cases} k_{12}^{(0)} & for\ t < t_1\ or\ t > t_2 \\ k_{12}^{(1)} & for\ t_1 \le t \le t_2 \end{cases}$	$\begin{cases} .0036 & for\ t < 220\ or\ t > 411 \\ .0043 & for\ 220 \le t \le 411 \end{cases}$
$g_{on} \rightarrow g_{off}$	Gene Inactivation	k_{21}	0.1423
$g_{on} \rightarrow g_{on} + mRNA_{Nuc}$	Transcription	k_m	0.1153
$mRNA_{Nuc} \rightarrow mRNA_{Cyt}$	Translocation	k_T	2.9861
$mRNA_{Nuc} \rightarrow \varnothing$	Degradation	γ_N	0.0458
$mRNA_{Cyt} \rightarrow \varnothing$	Degradation	γ_C	0.0458

(1)

In this description the rate of gene activation takes two values: $k_{12}^{(0)}$, which corresponds to the steady state activation in the absence of LPS activation and $k_{12}^{(1)}$, which corresponds to the activation rate for a period of time after LPS activation. Each of the rate parameters $\{k_{12}^{(0)}, k_{12}^{(1)}, k_{21}, k_m, k_T, \gamma_N, \gamma_C\}$ as well as the two times $\{t_1, t_2\}$ are treated as unknown values. For a given set of parameters, it is simple simulate the stochastic dynamics using a stochastic simulation algorithm[19].

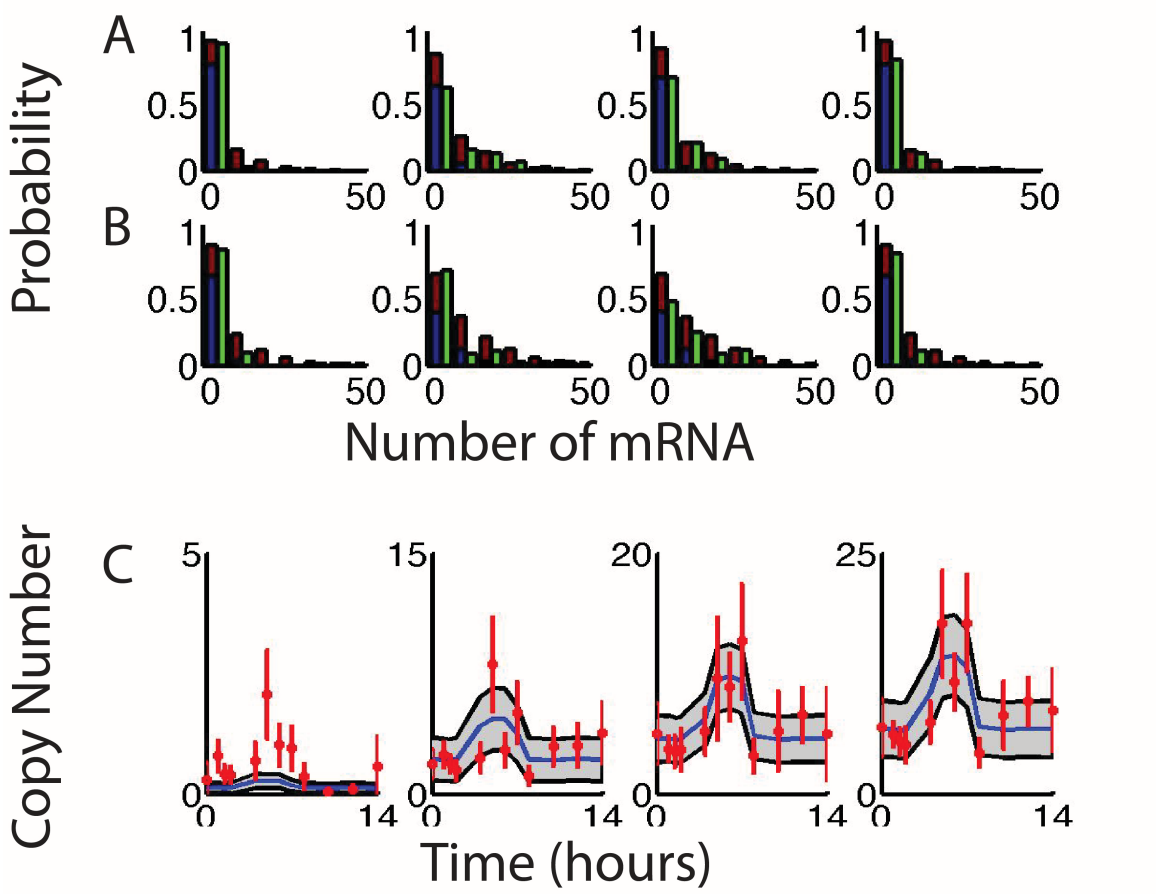

6

Figure 5 – A) Measured (green) and predicted (blue) distributions of nuclear IL1α mRNA production in response to LPS at {0,300,420,840} minutes (left to right). The uncertainty in model predictions is plotted in red. B) Measured (green) and predicted (blue) distributions of cytoplasmic IL1α mRNA production in response to LPS at {0,300,420,840} minutes (left to right). The uncertainty in model predictions is plotted in red. C) Time-resolved transcription dynamics for transcription sites, free nuclear mRNA, free cytoplasmic mRNA, and total cellular mRNA (respectively left to right). Red squares correspond to the measured mean expression level at a given time point. The blue line corresponds to the best model for the transcriptional dynamics after 100 generations of a genetic algorithm search. The shaded region is the expected uncertainty (from the model), and the error bars correspond to the uncertainty from the measurements. In each case, the errors are two standard deviations.

To estimate the parameters, we conduct a simple genetic algorithm search, in which we randomly generate 40 sets of parameters per generation, run 100 stochastic simulations for each set, compare to the data, and finally select the best parameters sets from which to generate new parameters. We repeat this process for 100 generations. After the parameters have been identified from the mean mRNA behaviors, we use these to predict the distributions of mRNA in the nucleus and cytoplasm, as shown in Figure 5a-b. The best parameter set after 100 generations (given in the last column of eq. 1) is used to plot the mean numbers of transcription sites, nuclear mRNA and cytoplasmic mRNA as a function of time in Figure 5c.

3.3 Co-localization of two color GAPDH mRNA

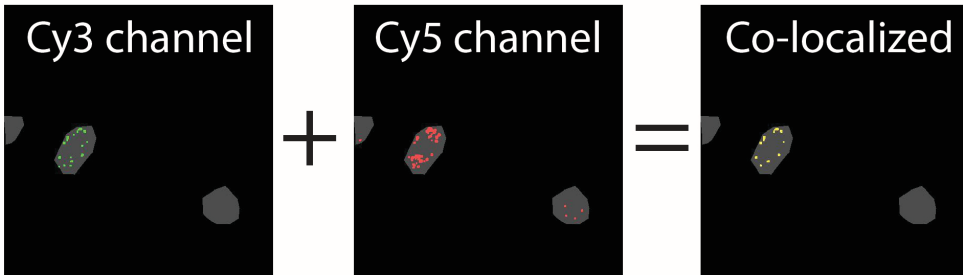

Figure 6 – Representative merged maximum Z-projection images of GAPDH mRNA labeled with both Quasar 560 (Cy3 channel) and Quasar 670 (Cy5 channel). The fluorescence spots are identified in three dimensions by our spot finding software and then the localized spots are determined by a hierarchal search of shared volume fraction through all spots in both channels.

To verify our ability to detect smaller RNA targets, such as bacterial sRNA, we imaged a split probe set hybridized to GAPDH mRNA. The probe set is designed such that the number of probes hybridized to an individual GAPDH mRNA transcript in both channels is close to the number of probes (approximately 15) that we anticipate hybridizing to a 337 nucleotide sRNA found in both *Yersinia Pseudotuberculosis* and *Yersinia Pestis* [20]. Multiple Z-stacks were taken in four color channels. The white light channel is used to locate individual cells in each Z-stack, the DAPI channel is used to localize the nucleus of each cell in 3D, a Cy3 channel is used to localize the Quasar 560 labeled portions of GAPDH mRNA in 3D, and a Cy5 channel is used to localize the Quasar 670 labeled portions of GAPDH mRNA in 3D. Figure 6 shows representative maximum Z-projection images from Z-stacks corresponding to the white light, Cy3, and Cy5 channels. Because we localize each mRNA spot in three dimensions, we are able to determine co-localized fluorescence spots as outlined in Section 2.4. The percentage of co-localization in Figure 6 is greater than 75 percent. Our typical percentage co-localization throughout a population is a bi-modal distribution, either greater than 75 percent or less than 10 percent. We attribute this to an imperfect hybridization procedure for this split probe set. Because each probe set only consists of 16 probes, we are continuing to develop procedures to limit non-specific binding and reduce false positives. Given our current success, we are confident in imaging sRNA targets with probe sets containing as few as fifteen probes.

4. DISCUSSION

In this study, we have used single-molecule techniques to measure the activation of IL1α mRNA transcription upon induction by LPS. By measuring mRNA levels at many points in time, we have collected quantitative data, which has allowed us to fit a predictive model for of IL1α activation. Our data show a clear increase in transcription beginning at about 300 minutes after LPS stimulation (Figure 4). In our model, this corresponds to a LPS-enhanced activation of transcription sites, which begins at about 220 minutes and which lasts for about 90 minutes (Figure 5c). Our model also captures the spatial aspects of mRNA translocation from the nucleus to the cytoplasm, and the degradation of mRNA. Most importantly, the model is capable of predicting cell-to-cell heterogeneity in mRNA copy numbers in the nucleus and cytoplasm (Figure 5a-b). By using these probability distributions to inform our model selection and identification, we are able to reach a much greater level of predictive understanding, which can guide future experiments acquired under new conditions. Without precise quantification of single mRNA transcripts, such understanding would be more limited. For example, the use of GFP-fusion would not only hide mRNA translocation dynamics, but would also introduce extraneous maturation dynamics to the process. One could still obtain spatio-temporal information and probability distributions for the protein complex, but with much less insight into the endogenous mRNA lifecycle. Figure 5 shows the end result of this down-selection for IL1α mRNA stimulation by LPS.

Figure 6 shows the result of optimizing the hybridization process for two 16-probe smFISH probe sets hybridized to individual GAPDH mRNA. We find that background noise for the Quasar 570 labeled probes is significantly higher than the Quasar 670 labeled probes, indicating that the correct label for a single small probe set is Quasar 670. By co-localizing these probe sets onto individual GAPDH mRNA transcripts and comparing these results to the average copy

number for GAPDH transcripts for the full smFISH probe set (32 probes) we find that we are counting greater than ninety percent of GAPDH mRNA transcripts for samples that have substantial co-localization. These results verify that the experimental apparatus and data analysis tools we have developed are capable of imaging probe sets as small as 16 probes, opening the door to direct detection of sRNA by the smFISH method.

5. CONCLUSION

In order to elucidate the role of small RNA in cellular regulation, we first must develop the necessary tools to probe how sRNA fits into the central dogma of genetic expression. Some of this work has been completed at the ensemble level, such as identification of new sRNA and genetic manipulation to test the effect of deleting a key sRNA[20]. Here, we present new tools to investigate this open question through the analysis, spatial localization, and counting of single mRNA transcripts in a large number of cells using a custom controlled microscope that can acquire and analyze this data with minimal user interaction. By integrating experimental single-cell measurements and discrete stochastic modeling, we were able to identify a simple, yet predictive toy model that quantitatively captures cell-to-cell heterogeneity in gene activation and transcription site formation, as well as transcript production, translocation and degradation.

We have demonstrated the ability to measure and model a regulatory pathway, the Interluekin 1-alpha cytokine, at the single mRNA transcript level. By designing a split probe set, we have shown our ability to detect probe sets as small as 16 singly labeled probes in a high-throughput manner, as well as co-localize two separate sets of fluorophores present on a single mRNA transcript.

ACKNOWLEDGMENTS

This work was supported through Los Alamos National Laboratory Directed Research and Development (LDRD) and was performed at the Center for Integrated Nanotechnologies, a U.S. Department of Energy, Office of Basic Energy Sciences user facility at Los Alamos National Laboratory (Contract DE-AC52 06NA25396) and Sandia National Laboratories (Contract DE-AC04-94AL85000).

REFERENCES

[1] A. M. Femino, F. S. Fay, K. Fogarty *et al.*, "Visualization of Single RNA Transcripts in Situ," Science, 280(5363), 585-590 (1998).

[2] H. M. T. Choi, J. Y. Chang, L. A. Trinh *et al.*, "Programmable in situ amplification for multiplexed imaging of mRNA expression," Nat Biotechnol, 28(11), 1208-1212 (2010).

[3] J. Lu, and A. Tsourkas, "Imaging individual microRNAs in single mammalian cells in situ," Nucleic Acids Res, 37(14), e100 (2009).

[4] A. Raj, P. van den Bogaard, S. A. Rifkin *et al.*, "Imaging individual mRNA molecules using multiple singly labeled probes," Nat Meth, 5(10), 877-879 (2008).

[5] A. Katranidis, D. Atta, R. Schlesinger *et al.*, "Fast Biosynthesis of GFP Molecules: A Single-Molecule Fluorescence Study," Angew Chem Int Edit, 48(10), 1758-1761 (2009).

[6] Z. Waks, A. M. Klein, and P. A. Silver, "Cell-to-cell variability of alternative RNA splicing," Mol Syst Biol, 7, 506 (2011).

[7] I. Topalidou, and M. Chalfie, "Shared gene expression in distinct neurons expressing common selector genes," P Natl Acad Sci USA, 108(48), 19258-19263 (2011).

[8] L. So, A. Ghosh, C. Zong *et al.*, "General properties of transcriptional time series in Escherichia coli," Nat Genet, 43(6), 554-560 (2011).

[9] J. D. Shih, Z. Waks, N. Kedersha *et al.*, "Visualization of single mRNAs reveals temporal association of proteins with microRNA-regulated mRNA," Nucleic Acids Res, 39(17), 7740-7749 (2011).

[10] M. Harterink, D. h. Kim, T. C. Middelkoop *et al.*, "Neuroblast migration along the anteroposterior axis of C. elegans is controlled by opposing gradients of Wnts and a secreted Frizzled-related protein," Development, 138(14), 2915-2924 (2011).

[11] K. Chen, and N. Rajewsky, "The evolution of gene regulation by transcription factors and microRNAs," Nat Rev Genet, 8(2), 93-103 (2007).

[12] M. Ghildiyal, and P. D. Zamore, "Small silencing RNAs: an expanding universe," Nat Rev Genet, 10(2), 94-108 (2009).
[13] L. He, and G. J. Hannon, "MicroRNAs: small RNAs with a big role in gene regulation," Nat Rev Genet, 5(7), 522-531 (2004).
[14] O. Hobert, "Gene Regulation by Transcription Factors and MicroRNAs," Science, 319(5871), 1785-1786 (2008).
[15] E. Masse, N. Majdalani, and S. Gottesman, "Regulatory roles for small RNAs in bacteria," Curr Opin Microbiol, 6(2), 120-124 (2003).
[16] S. Mukherji, M. S. Ebert, G. X. Y. Zheng *et al.*, "MicroRNAs can generate thresholds in target gene expression," Nat Genet, 43(9), 854-859 (2011).
[17] K. Papenfort, and J. r. Vogel, "Regulatory RNA in Bacterial Pathogens," Cell Host Microbe, 8(1), 116-127 (2010).
[18] R. Sedgewick, [Algorithms in C, 3rd Edition,] Addison-Wesley, 11-20 (1998).
[19] D. T. Gillespie, "Exact stochastic simulation of coupled chemical reactions," Journal Phys Chem, 81(25), 2340-2361 (1977).
[20] J. T. Koo, T. M. Alleyne, C. A. Schiano *et al.*, "Global discovery of small RNAs in Yersinia pseudotuberculosis identifies Yersinia-specific small, noncoding RNAs required for virulence," P Natl Acad Sci USA, 108(37), 709-717 (2011).